

GeoOLSR: Extension of OLSR to support Geocasting in Mobile Ad Hoc Networks

Volker Köster, Andreas Lewandowski, Dennis Dorn and Christian Wietfeld

Communication Networks Institute (CNI)

TU Dortmund University, Germany

Email: {Volker.Koester|Andreas.Lewandowski|Dennis.Dorn|Christian.Wietfeld}@tu-dortmund.de

Abstract—Safety critical applications of IEEE802.15.4 networks require autonomous network reconfiguration and dynamic meshing in case of node failures or changing environmental influences. This paper demonstrates the application of Ad hoc On Demand Distance Vector (AODV) and Optimized Link State Routing (OLSR) on IEEE802.15.4 nodes based on an IP layer. The modular concept leads to the proposed extension of Optimized Link State Routing (OLSR) protocol to provide location-based services and addressing inherently in the protocol design. We demonstrate the changes in message flows and information exchange that are necessary to develop a geo-implementation of OLSR, which we call GeoOLSR throughout this paper. For performance evaluation, we will first examine mobile ad hoc relevant metrics like time delay, maximum throughput and generated overhead. Furthermore, the lifetime of the novel node architecture is evaluated in comparison to the ordinary IEEE802.15.4 configuration and IEEE802.11. Finally, the real-world protocol behavior of GeoOLSR is shown for different mobility speeds by using realistic ray tracing for modeling the physical transmission in a harsh industrial environment. Thus, it is proven by results that GeoOLSR is able to support both IP enabled unicast traffic and geographical addressing even in resource constrained networks like IEEE802.15.4.

Keywords-Geocasting; OLSR; AODV; IEEE802.15.4; Ray Tracing.

I. INTRODUCTION

The application of wireless sensor networks (WSNs) or mobile ad hoc networks (MANETs) based on IEEE802.15.4 in safety-critical processes requires a fault tolerant network design, which supports autonomous reconfiguration [1]. Recent developments in the area of Wi-Fi networks propose meshing algorithms on ISO/OSI layer 3 like the reactive Ad hoc On demand Distance Vector (AODV) Routing [2] or the proactive Optimized Link State Routing (OLSR) [3], which are capable to update communication paths in case of failures and mobility of network nodes. In contrast to that, original IEEE802.15.4 networks rely on topologies like star or cluster tree, in which failures of single nodes can isolate even complete network trails.

Therefore, the IEEE task group 802.15.5 *Mesh Networking* currently examines necessary mechanisms that are designed for the physical (PHY) and medium access control (MAC) layer. In order to enable a flexible network setup for different application scenarios within heterogeneous networks, we analyze multihop forwarding via IP routing

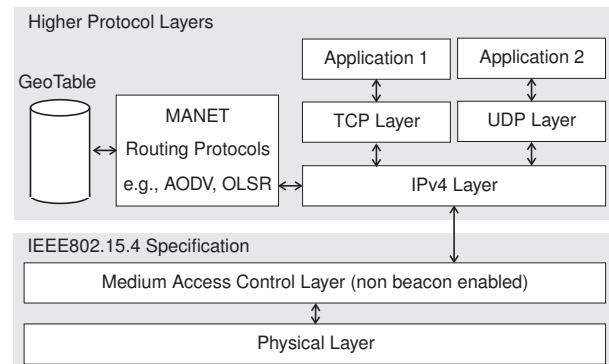


Figure 1. The extended Layer Model of our proposed architecture to support IP enabled unicast traffic and geographical addressing in IEEE802.15.4

mechanisms (on layer 3 – also known as *Route-over* [4]). We propose a node design (see Figure 1), which includes an IPv4 layer – instead of utilizing the ZigBee protocol stack [5]. The integration of the IP protocol for WSNs is proposed in [4] and [6]. The big advantage of these approaches is the seamless integration into the Internet. In [7], it has been shown that the implementation of a tiny TCP/IP protocol is feasible for the integration on low power devices, such as IEEE802.15.4 without major changes of the PHY- or MAC layer. Following these approaches, this paper demonstrates the application of OLSR and AODV routing schemes as proposed in [8] by applying a peer-to-peer network topology. Here, every node is assumed to operate as a router and uses CSMA/CA channel access.

Besides an easy integration of IEEE802.15.4 nodes into preexisting infrastructures, diversified application domains are one key performance indicator of MANETs. Thus, there is an increasing need for a simultaneous support of geographical addressing to realize e.g., location based messaging and alarming. As an extension to [1], it is an objective of this paper to show an extension of OLSR – which will be called GeoOLSR throughout this thesis – to build up a routing protocol, which supports unicast (IP-based) as well as geographical multicast communication inherently. Therefore, a slight modification to the original protocol architecture is made by adding an additional routing table (called GeoTable), which contains positions of reachable nodes (cf. Figure 1). The major benefit of using

a proactive routing protocol like OLSR is the periodical exchange of routing information in discrete time intervals. This enables knowledge of a node's last position even in case of malfunctions. In contrast to that, on-demand routing mechanisms only search for a new route prior a specific communication request.

The work is part of a research project with one of the world's largest steel fabricants ThyssenKrupp Steel. They will install the presented solution to increase the security of the factory employees in case of emergency. The developed solution is integrated in a gas sensor network, which consists of stationary and mobile equipment. Hence, not only factory employees, but also first responders profit from this solution, as they do not have to carry additional devices for navigating through the incident scene. Thus, this work presents several major contributions:

- Demonstration of the general applicability of meshed network approaches within IEEE802.15.4 networks by implementing our IP enabled sensor node architecture based on the physical layer of IEEE802.15.4 using a peer-to-peer enabled CSMA/CA MAC layer.
- Introduction of a detailed performance evaluation of AODV and OLSR in IEEE802.15.4 networks.
- Proposal of an OLSR extension, which enables geocasting as well as IP-based unicast messages combined with high node mobility support.
- Comparison of different geocast routing protocols e.g., Location Based Multicast (LBM), flooding GRID, ticket GRID and GeoTORA with GeoOLSR.
- Evaluation of the influence of different moving speeds and patterns on GeoOLSR.
- Brief identification of the resulting overheads of GeoOLSR compared to OLSR.
- Analysis of the proposed GeoOLSR protocol in a real-world scenario considering realistic radio channel effects by application of the Actix Radiowave Propagation Simulator (RPS) [9], which includes a high-precision 3-dimensional CAD drawing of the application scenario within the steel production plant.

This paper is organized as follows. Section II discusses related works. Afterwards we demonstrate the design of the new node in Section III in detail, before the implementation of the applied simulation model in OMNeT++ 4.0 is shown as well as details of the simulation measurements in Section IV. After that, we illustrate the protocol extension of GeoOLSR within Section V by presenting necessary changes in message flows and information exchange to realize a geo-implementation of OLSR, followed by corresponding analysis in Section VI. Performance evaluations via OMNeT++ simulation together with a sophisticated PHY layer model based on the ray tracing tool RPS are presented in Section VII. Finally, Section VIII draws conclusions.

II. BACKGROUND AND RELATED WORK

In this Section, we will give a brief introduction into state-of-the-art routing protocols divided into four groups – unicast MANET protocols, geographical multicast protocols, mobile agents protocols and hierarchical routing protocols.

A. Unicast Mobile Ad-Hoc Network Protocols

Linking an IP address with a geographical location has been of interest for quite some time already. On the other hand, there has also been significant research to increase network redundancy in general, based on unicast routing protocols for MANETs, in which all mobile hosts typically behave as routers. A route between a pair of nodes in a MANET may go through several other mobile nodes. Due to the mesh network approach these routes may vary when nodes change their locations. Many attempts have been made on MANET protocols [2], [3], [10]. There are two major types of networking protocols defined in the literature for this application field [11]:

- *Proactive routing*: A node manages the whole network topology in a periodically updated routing table, which causes additional traffic.
- *Reactive routing*: The route is determined when a packet has to be transmitted. Hence, the delay for a single packet transmission is higher in comparison to proactive routing; however, the additional traffic for route maintenance is minimized.

In the following paragraphs, basic principles of OLSR as a proactive and AODV as a reactive routing scheme are described in detail.

OLSR

The Optimized Link State Routing is specified in the RFC 3626 [3]. Simulative and experimental performance evaluation on Wi-Fi devices is presented in [11]. *Route table calculation* is done by topology information, which is gathered from topology control messages (TCM). If a node generates its neighbor list, the TCMs are transmitted through the network. A node is defined as a neighbor, if a bi-directional physical connection between two nodes is available. Following RFC 3626, OLSR communicates using a unified packet format for all data related to the protocol. This is meant to facilitate extensibility of the protocol without breaking backwards compatibility. This also provides an easy way of piggybacking different "types" of information into a single transmission like geographic data in the field of GeoOLSR. A RFC 3626 standard implementation is embedded in IPv4. The basic layout of any packet in OLSR consists of an OLSR header, which includes three types of messages:

- *OLSR-Hello* To perform link sensing, neighborhood detection and Multi-Point-Relay (MPR) selection, Hello messages are exchanged between 1-hop neighbors periodically. This message is sent as the data-portion of

the general packet format with the "Message Type" set to HELLO_MESSAGE, the Time-to-live field set to one and Vtime set accordingly to the value of NEIGHB_HOLD_TIME.

- *OLSR-Topology-Control* The link sensing and neighbor detection part of the OLSR protocol basically offers a neighbor list in each node, which contains a list of neighbors to which a direct communication is possible. In combination with the packet format and forwarding mechanism, an optimized flooding through Multi-Point-Relays (MPRs) is implemented. This mechanism is based on the OLSR-Topology-Control (TC) message format, which disseminates topology information through the whole network.
- *OLSR-Multiple-Interface-Declaration* The OLSR-Multiple-Interface-Declaration (MID) message is used to map more than one IP address to one node. Therefore, all interface addresses other than the main address of the originator node are put into the MID message.

The use of multipoint relays (MPRs) reduces the network load by concentrating the traffic on dedicated nodes. The speed of topology update processes can be regulated by varying Hello and TC intervals. The main performance indicators of OLSR are summarized in Table I. The willingness for a MPR is defined by the remaining battery power of the node.

Table I
PARAMETERIZATION OF OLSR NODES

Hello Interval	inter-arrival time of hello packets
Hello Jitter	maximum deviation from the hello interval
TC Interval	inter-arrival time of TC packets
TC Jitter	maximum deviation from the TC interval
Hello Timeout	maximum timeout of hello messages until the node is removed from the neighbor list
Willingness	willingness of a node to act as MPR

To reduce the negative influence of packet losses due to high mobility in OLSR, Benzaid et al. proposed a new method of integrating fast mobility in the OLSR protocol [12].

AODV

The Ad hoc On Demand Distance Vector routing is specified in RFC 3561 [2].

An application for IEEE802.15.4 networks has been proposed by [13] without applying an IP layer. Each node operates as a router and determines point to point connections on demand without periodical updates. Thereby, memory and energy demand is optimized for battery driven mobile devices and the additional network load is minimized. An included sequence number avoids the count-to-infinity routing problem [2]. In contrast to other routing protocols, the quality of a connection is determined by the actuality and not

Table II
PARAMETERIZATION OF AODV NODES

Active Route Timeout	defines the validness of a route
Hello Interval	defines the inter-arrival time of hello packets
Allowed Hello Loss	defines the maximum hello packet loss until a route is deleted
Delete Period	defines the limit of route from node A and B to D, if node A has deleted the route
Net Diameter	maximum number of hops between two nodes
Node Transversal Time	estimated for a 1-hop transmission
Net Transversal Time	2* Node Transversal Time * Net Diameter
Path Discovery Time	2* Net Transversal Time
RREQ Retries	number of attempts for route determination

by the length of the path. The main configuration parameters of AODV are summarized in Table II.

B. Geographical Multicast Protocols

In addition to the work mentioned before, there has also been significant work on multicasting based on the location of the particular nodes. Several approaches have been proposed [14] [15]. The schemes for multicasting can be broadly divided into two types: flooding-based schemes and tree-based schemes. Flooding-based schemes (like Location-Based Multicast [16]) do not need to maintain as many network states as tree-based protocols. On the other hand, flooding-based schemes can potentially deliver multicast packets to many nodes that are currently outside the location, which is energetic inefficient. Tree-based schemes (cf. GeoTORA [14] and GeoGrid [15]) reduce the amount of sent messages. However, a higher overhead is needed to maintain the network's tree.

C. Mobile Agents Protocols

Other routing schemes are based on mobile agents and are inspired from social insects' behavior [17]. One of the main ideas of ant algorithms is the indirect communication of a colony of agents, based on so called pheromone trails. Pheromones are used by real ants for communication purposes. The ants know the other ants' paths by the pheromone trails, and the amount of pheromone on a trail reflects its importance.

D. Hierarchical Routing Protocols

Besides the location based routing approach some attempt has been made to support a routing algorithm that integrates geo-coordinate and table-driven IP addressing [18]. This routing protocol called "GeoLANMAR" uses link-state routing in a local scope and geo-routing for out-of-scope packet forwarding. The protocol keeps track of the routes to destinations up to a certain distance away from the source whereas the geo-routing scheme applied in GeoLANMAR is used to route packets to the remote landmark nodes outside the local scope.

III. DESIGN OF AN IP-ENABLED WIRELESS SENSOR NODE

The simulation model is implemented in the discrete, event-based network simulator OMNeT++ [19] and the INET framework. Figure 1 shows the implementation of the communication node. The IEEE802.15.4 physical layer implementation [20] of OMNeT++ is used for the proposed extensions. By using the IP layer, also the existing UDP and TCP protocol implementations of the INET framework can be evaluated for new services. An additional 20 byte IP header and an 8 byte UDP header decrease the overall capacity. But 74 byte payload are left, which is enough for sensor monitoring applications and additional services, as the maximum payload size of the messages in this application area is usually inherently small.

In order to highlight the generated overhead in comparison to a conventional IEEE802.15.4 network, the resulting throughput is measured in a simple point-to-point scenario. The new node is operating with AODV in the first case and OLSR in the second case. For system startup, a time off of 10s is set before measurement values are captured. The applied parameters of the meshing protocols are summarized in Table III.

Table III
PARAMETERIZATION OF THE TEST SCENARIO

Traffic profile	OLSR settings	AODV settings
74Byte (UDP Payload) every 30ms $\approx 19.73\text{kbit/s}$	Willingness = 3 Hello Interval = 1s TC Interval = 2s MID Interval = 2s	Active Route Timeout = 6s Hello Interval = 1s Allowed Hello Loss = 2 Delete Period = 10s Net diameter = 2 Hops Node transversal time = 40ms RREQ Retries = 2

This parameterization is assumed for all following performance evaluations. The values for the hello interval (HI) of OLSR and AODV are chosen equally for an optimal comparison.

Figure 2 depicts the resulting overhead generated by the new implementation. About 10kbit/s overhead must be calculated for the application of IP-based meshing protocols in a simple point-to-point scenario. The following performance evaluation will also clarify the scalability up to an 8 hop scenario.

IV. EVALUATION OF THE NOVEL PEER-TO-PEER APPROACH

To demonstrate general feasibility of the novel architecture, we first evaluate important performance indicators like end-to-end transmission delay, goodput during handover processes, handover delay and achievable throughputs in an OMNeT++ simulation environment. However, typical PHY layer issues like CCA delay [21] or co-channel interferences [22] are neglected at this point. Figure 3 depicts a hidden-

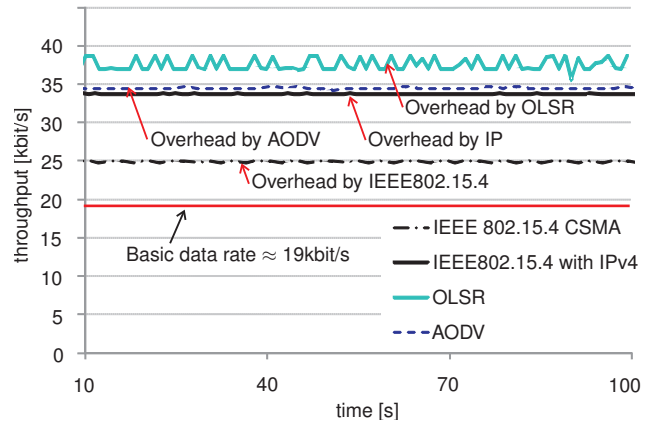


Figure 2. Comparison of network load between IEEE802.15.4 and the peer-to-peer implementation with applied AODV and OLSR routing algorithm for a simple point-to-point setup without mobility. The parameters of Table III are applied.

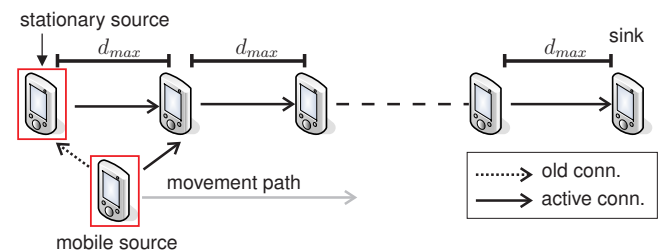


Figure 3. Hop-to-hop Scenario for Performance Evaluation

station hop-to-hop scenario. The setup consists of 8 hops placed in a hop distance of $d_{max} = 150m$, which represents the maximum radio range. Here, the string topology represents the worst case for OLSR due to the fact that the MPR forwarding becomes obsolete.

In each test, 74Byte packets (payload) are sent over the network from the stationary source each 30ms until the mobile node reaches the end of the playground. The performance evaluation is then structured as follows. First, we analyze the end-to-end delay in stationary node constellations before an analysis of handover scenarios between fixed network nodes and mobile nodes is achieved. Finally, the energy consumption is compared to an IEEE802.15.4 node implementation.

A. Evaluation of End-to-End Transmission Delay

The end-to-end delay is a good indicator to measure the response behavior and the real-time capability of the network. The parameterization of this experiment is described in Table III. The test is repeated 100 times, before the distribution function is calculated (cf. Equation 1) to determine the $\mu \pm 2\sigma$ interval, which includes 95.4% of all possible end-to-end delay values.

$$F(x) = \frac{1}{\sigma\sqrt{2\pi}} \int_{-\infty}^x e^{-\frac{1}{2}\left(\frac{t-\mu}{\sigma}\right)^2} dt \quad (1)$$

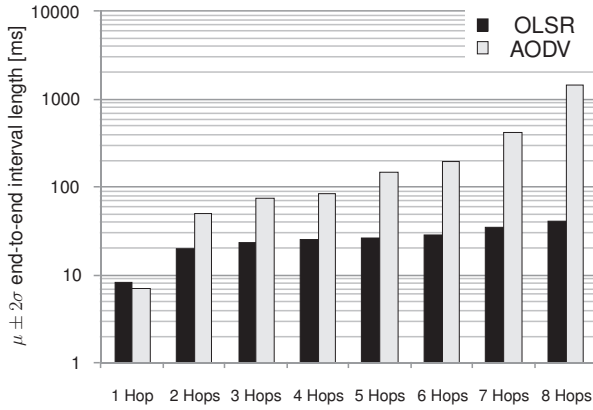


Figure 4. Interval length of the end-to-end delay for OLSR and AODV depending on the hop count for a stationary scenario depicted in Figure 3. The interval contains $\mu \pm 2\sigma$.

The results are assembled in Figure 4. The expected value for end-to-end delay of AODV is lower compared to OLSR in the one hop case, but in all other cases OLSR seems to be predominant. As a consequence, AODV exhibits an interval of [0 ms, 1435.1 ms] for the 8 hop case, which means that 95.4% of the examined cases fit into this interval, whereas OLSR features an interval of only [0 ms, 41.5 ms]. The high delay of AODV can be explained by the route determination process. With an *Active Route Timeout* of 6s and a *Delete Period* of 10s, routes are updated frequently assuming constant bitrate (CBR) traffic. The needed additional traffic for the route determination process rises with an increasing number of hops.

B. Performance Evaluation of Hand-Over Processes

As mobile sensors are regarded for typical application scenarios, fast handover processes are needed for reliable measurement transmission. The following experiments base on the measurement setup shown in Figure 3 with one moving source node transmitting data continuously (cf. Table III) over the next fixed node to the sink at a predefined constant speed for the mobility.

Figure 5 depicts the achievable goodput at different mobility speeds and hop counts for AODV. The reference line at 0 m/s shows the impact of the hop count on the maximum goodput. It can be seen that the throughput is almost constant until a hop count of 4. This finding correlates to the end-to-end delay for AODV depicted in Figure 4. A higher hop count decreases the achievable throughput, as the delay is nearly doubled from 4 Hops to 5 Hops. The same observation can be made for moving nodes. Here, the impact

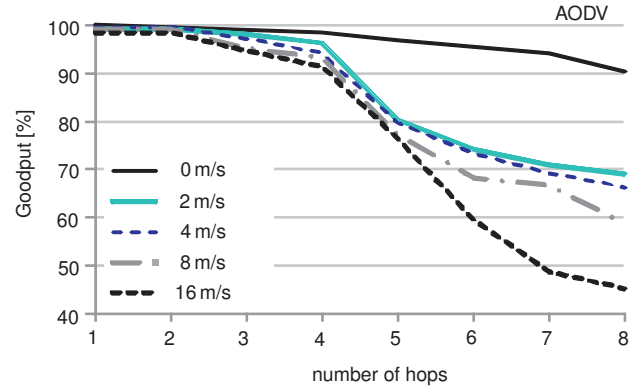


Figure 5. Goodput in percent for AODV depending on the hop distance to the sink with a mobile source transmitting to the next stationary node in range, which then forwards the information to the sink.

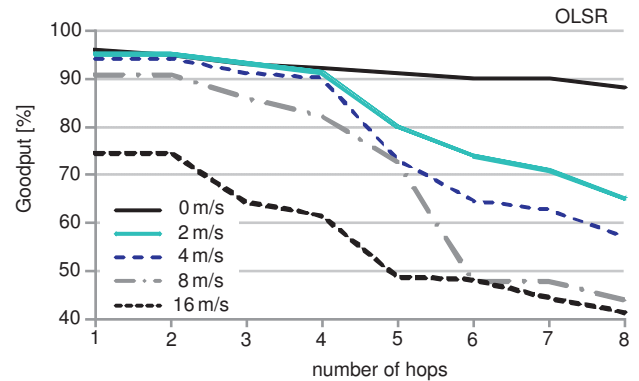


Figure 6. Goodput in percent of OLSR depending on the hop distance to the sink with a mobile source transmitting to the next stationary node in range, which forwards the information to the sink. Whilst performing route updates, the traffic is interrupted.

increases with higher mobility speeds, which is caused by the switching time of the accomplished handover processes.

For comparison of the performance of OLSR and AODV, Figure 6 depicts the achievable goodput for OLSR in the same network and measurement setup. OLSR starts at a lower goodput for the reference measurement at 0 m/s, as OLSR gathers – as a proactive routing scheme – the routing information for the entire network in advance, which takes about 6 seconds for this setup before the data transmission can start. As a consequence, higher overhead decreases the achievable goodput. Due to continuous traffic for route updates, the probability of collisions between OLSR control and data packets rises with the number of intermediate hops. As a consequence, the goodput decreases with a higher number of hops between source and sink.

The handover process itself decreases the goodput. A tradeoff between HI, which causes additional traffic (cf. Figure 2) and switching time for the handover has to be determined. Figure 7 depicts the OLSR handover delay for

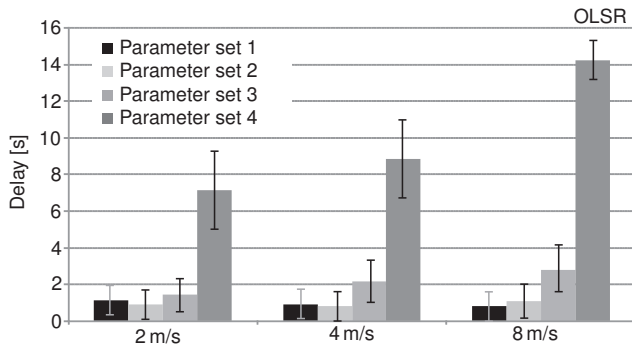


Figure 7. OLSR Handover delay for different mobility speeds and network configurations. *Parameter set 1*: Hello=1s, TC=1s, MID=1s; *Parameter set 2*: Hello=1s, TC=2s, MID=2s; *Parameter set 3*: Hello=2s, TC=5s, MID=5s; *Parameter set 4*: Hello=5s, TC=5s, MID=5s;

different network configurations and mobility speeds. It can be observed, that the main performance indicator is the hello interval (HI). As the HI is small, high speeds are supported by the network. As the HI is enlarged (e.g., to reduce the traffic overhead), the handover delay rises. This finding is comparable to a Wi-Fi study on OLSR [23], where the hello interval is described as the main performance parameter.

Analyzing performance related parameters of OLSR and AODV has been subject of many papers in recent years [23] [24]. However, each publication assumed IEEE 802.11 as the physical and data link layer protocols. To ensure a good comparability of our measurement results with the preexisting ones, we analyzed the mean values of the average throughputs and their standard deviations at varying speeds and parameter sets for both OLSR and AODV. Here, we let the mobile sink of Figure 3 move towards and away from the destination node and calculated the mean throughput for the whole distance. The results are depicted in Figure 8.

As expected, AODV outperforms OLSR in terms of mobility support due to periodical route maintenance of the pro-active routing algorithm. Considering the relative high throughput of our measurements and the shorter coverage areas of IEEE802.15.4, one can conclude that both findings are nearly congruent. In [23] the decrease of average throughput between a node speed of 0 m/s and 15 m/s varies from 25 % (HI = 1s, TC = 5s) to 26 % (HI = 2s, TC = 5s), whereas our simulative results show a difference of 28.59 % (HI = 1s, TC = 2s) and 25.97 % (HI = 2s, TC = 5s) respectively. The results for AODV comparison behaves equally, concluding that AODV still ensures a delivery ratio of more than 90 % even at high speeds for hop distances of up to 8 hops.

C. Energy consumption of meshed sensor nodes

Energy consumption is a critical issue for the design of wireless sensor nodes. IEEE802.15.4 standard divides the network in node classes, where *routers* and *coordinators* are always switched on for maintaining connection between nodes. The *end device* is the node class, which is designed

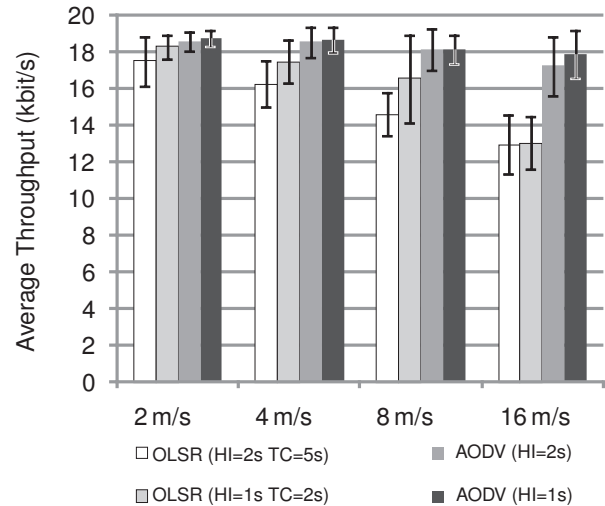


Figure 8. Comparison of the average throughputs of OLSR and AODV at different speeds

for transmitting sensor information. It operates with low en-

Table IV
PARAMETERIZATION OF BATTERY MODEL FOR TI CC2420 (IEEE802.15.4) AND MAX2822 (IEEE802.11B)

	TI CC2420 (Pout = 0dBm)	MAX2822 (Pout = +3dBm)
Supply Voltage	3V	3V
Standby-Mode Supply Current	1.38mA	25mA
Receive-Mode Supply Current	9.6mA	80mA
Transmit-Mode Supply Current	16.24mA	98mA
Rx Sensitivity	-95dBm	-85dBm

ergy consumption due to sleep phases and is only connected to a coordinator or cluster head. If the next higher node in hierarchy fails, the end device will be isolated from the rest of the network.

The applied battery model of OMNeT++ utilizes the parameterization shown in Table IV based on the data sheets of the *TI CC2420* [25] transceiver for IEEE802.15.4 and the *MAX2822* [26] for IEEE802.11b. Adaptive bit rate adjustment and changing power levels are neglected in this study; only worst case assumptions are evaluated, which means that always a transmit power of 0 dBm is applied for the CC2420 transceiver. Nevertheless, the parameter d_{max} is adjusted for maximum transmission range for Wi-Fi (250 m) and IEEE802.15.4 (150 m) respectively.

Following this parameterization, Figure 9 shows the energy consumption of applied AODV and OLSR in comparison to a regular IEEE802.15.4 end device and IEEE 802.11b.

Following this parameterization, Table V shows the simulated battery lifetimes of AODV and OLSR in comparison to a regular IEEE802.15.4 end device and IEEE 802.11b, which also applies both AODV and OLSR. We found that

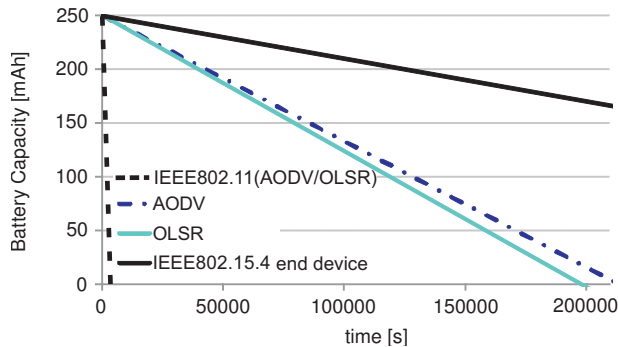


Figure 9. Lifetime of a 250mAh battery for different operation modes with the applied traffic pattern in Table III in a point-to-point scenario without mobility

Table V

BATTERY LIFETIME DEPENDING ON APPLIED ROUTING SCHEME FOR PARAMETERIZATION IN TABLE III FOR IEEE802.15.4 AND IEEE802.11

IEEE802.15.4 CSMA/CA	173h 36min
IEEE802.15.4 AODV	59h 20min
IEEE802.15.4 OLSR	54h 57min
IEEE802.11b (1Mbit/s) OLSR	55min
IEEE802.11b (1Mbit/s) AODV	55min

OLSR consumes slightly more energy than AODV in this configuration, which is caused by the relative high rate of control packets to maintain overall network topology information in each node. However, in comparison to Wi-Fi networks operating at 1MBit/s, the node lifetime is about 60 times higher for both cases.

V. GEOOLSR

In this chapter, we extend the original OLSR with geocasting capabilities. The main idea of GeoOLSR is shown in Figure 10. Each node within the whole network administrates a modified routing table, which contains the IP address and position of every neighbor node. This enables a direct mapping of position information to regular IP addresses, which facilitates efficient forwarding of location based information. However, the performance of maintaining moving nodes in the routing table strongly depends on the update process, which is regulated by the periodic emission of OLSR control packets. Hence, relevant parameters have to be optimized for a sophisticated use within wireless sensor networks. We assume that each node participating in the entire network is aware of its position, which may be expressed by absolute or relative coordinates to a given fixed-point. For performance analysis, we use a random mobility model.

A. Extension of OLSR with Geocasting Capabilities

Due to the periodical exchange of Hello and Topology-Control messages in OLSR networks (cf. Section II), the key assumption is to use these two packet formats to broadcast position information as well as regular IP-based topology

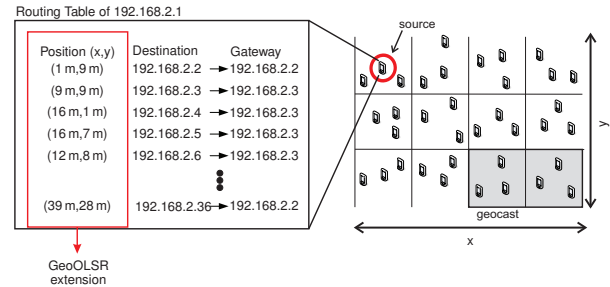


Figure 10. Basic idea of extending OLSR to map location based services on IP-based unicast messaging

information within the network. The new *GeoOLSR Hello* frame extends the standard OLSR Hello packet with an additional header as follows:

- *Type (1 Byte)* The type field indicates the applied position format e.g., GPS-RMC (GPS-Recommended Minimum Sentence C), GPS- or Cartesian coordinates (8 Byte floating point for each x- and y-coordinate).
- *Length (2 Bytes)* Due to the variable length of GPS payload, this field denotes the byte length of the additional (position) payload.
- *Reserved (1 Byte)* This field enables future extensions like geo-referenced rescue maps, situation photos etc.

In contrast to that, *Topology Control (TC)* messages are used to broadcast information beyond 1 hop distances. TC messages are only forwarded by Multi Point Relays (MPRs), which are used to decrease the number of transmissions required for OLSR related control mechanisms. To broadcast position information of each node participating in the considered network, the TC message format also has to be adapted to GeoOLSR. In contrast to the *GeoOLSR Hello* packet, a *GeoOLSR TC* message may include more than one node position. Hence, a separate position data header is denoted for each advertised neighbor's main address. This additional header also includes a *Type*, *Length* and *Reserved* field. However, the two packet formats *GeoOLSR Hello* and *GeoOLSR TC* are only used during initialization. After network setup phase, recently joined or moving nodes can be added or updated to the topology by using the proposed GeoOLSR frames *Fast Hello* and *Fast TC*, which will be explained later in this section. The application of the modified *GeoOLSR Hello* and *TC* packets only at network startup enables a fast convergence to the original OLSR algorithm without changes on specific OLSR route and MPR selection. As a consequence, there will not be any position related update after initialization when there is no node mobility within the network. However, each node needs to maintain a node list, in which the coordinates are saved together with the corresponding IP addresses, which enables a mapping of position information to regular IP addresses.

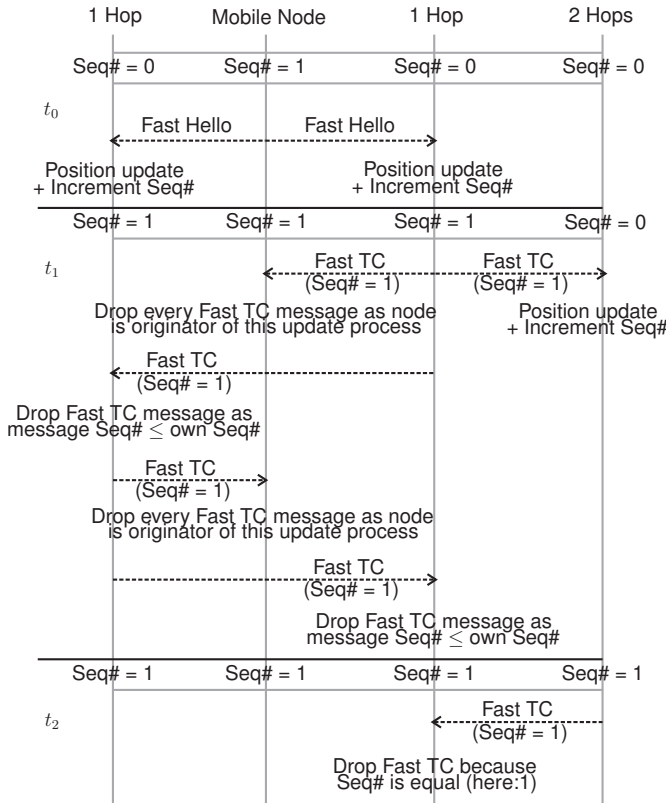


Figure 11. Update Process exchanging Fast Hellos and Fast TCs

In order to enable accurate position updates at high node mobilities even in far-off nodes, we modified the Fast OLSR approach of Benzaid et al. [12] (cf. Figure 11).

In this paper, we also use fast hello messages to track the fast moving nodes' motion sufficiently. To achieve this goal, a moving node (or a node, which recently joined the regarded network) emits position update packets to its direct neighbors at a high frequency in form of *GeoOLSR Fast Hello* messages. In contrast to the original Fast OLSR approach, we do not apply *GeoOLSR Fast Hellos* to increase overall network redundancy, but rather accuracy of position information. That means we reduce fast hello message fields to a minimum, including only position data. Here, no additional IP address of the sending node is required as this information is already denoted in the regular OLSR header. The frequency of *GeoOLSR Fast Hello* emission is determined by the new parameter *Fast Hello Interval*. Thus, our *GeoOLSR Fast Hello* packet format is developed for resource constrained IEEE802.15.4 nodes and allocate a minimum of payload.

In contrast to *GeoOLSR Fast Hello* messages, *GeoOLSR Fast TC* messages are used to transfer position updates to far-off nodes within the network. In contrast to regular Topology-Control messages of OLSR, *GeoOLSR Fast TC* messages are distributed using broadcast. To limit the

broadcasts after each node has received the updated position, a 2 Byte sequence number is integrated in the *GeoOLSR Fast TC* message format besides the IP address and the new position of the moving node. This allows a fast distribution of position updates without profound changes of the OLSR protocol. An example of the update process is shown in Figure 11. At the beginning the mobile node recognizes that it is moving and thus sends *GeoOLSR Fast Hellos* to all neighboring nodes. All nodes, which receive a *GeoOLSR Fast Hello* update the corresponding position information of their geocast table. The explicit assignment is achieved by fixed IP addresses. Each geocast table entry is equipped with an additional sequence number that is incremented when a position update is performed. After that, another *GeoOLSR Fast TC* message is generated and broadcasted, which includes the recently updated position, the IP address of the moving node and the incremented sequence number. Every node, which receives a *GeoOLSR Fast TC* - except the originator of the update process - checks if the packet's sequence number is larger than its own. If true, the new position is updated and forwarded, otherwise the packet is discarded. In Table VI the most important *GeoOLSR* parameters and their behavior on network performance are shown.

 Table VI
 MAIN PARAMETERS OF GEOOLSR

Hello Interval	Emission interval of <i>GeoOLSR Hello</i> messages.
TC Interval	Emission interval of <i>GeoOLSR TC</i> messages.
Fast Hello Interval	Emission interval of <i>GeoOLSR Fast Hello</i> messages.
Network Init Time	Based on the network size this value limits the time until <i>GeoOLSR Hello</i> and <i>TC</i> messages are used for position updates. After Network Init Time only <i>GeoOLSR Fast Hellos</i> and <i>GeoOLSR Fast TCs</i> are used for position updates.

B. Broadcasting data using geocast regions

A general problem that occurs using location based services in a Wireless Sensor Network (WSN) is the limited payload of IEEE802.15.4 Medium Access Control (MAC) layer. Thus, the MAC layer, on which an IP and an UDP layer are based, offers only a maximum payload of 74 Byte.

Assuming many nodes to be situated in the considered geocast region, it is not advisable to route the file to each destination node separately. Therefore, the packets are first delivered to one or more gateways. After that, they will be broadcasted within the corresponding geocast region. This method is shown in Figure 12. Due to the proactive approach of OLSR, the source node has a full overview over all node positions in the entire network. Thus, it can calculate, which nodes are situated in the destination region. Then, the source node determines a node, which is placed most closely in the middle of the desired geocast region.

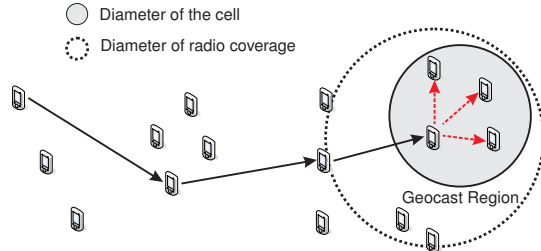


Figure 12. Broadcasting location based data via GeoOLSR

To ensure an adequate connectivity within the geocasting regions, the cell sizes must be smaller than the radio coverage of the nodes. If the resulting coverage area does not overlap fully with the desired destination region, two or more gateway nodes must be selected by the corresponding source node. Furthermore, the particular recipients are always aware of their own positions and may drop data packets, if the node is currently situated outside the desired geocast region.

The amount of gateways depends on the size of the considered geocast region and the cell size, which is strongly influenced by particular application environment properties (i.e., outdoor or indoor). Furthermore, environmental conditions influence the radio coverage and have to be estimated with certain channel models in advance. The selection of the cell size has a high impact on the connectivity between neighboring grids. Hence, a smaller cell size means more number of gateways in the network, resulting in a higher overhead of delivered packets and decreased battery lifetime especially in WSNs. However, this discussion has already been made in the GeoGrid thesis of Wen-Hwa Liao et al. (cf. [15]) and is not part of the present work.

VI. GEOOLSR PROTOCOL ANALYSIS

To evaluate the performance of GeoOLSR, we implemented a full mesh capable node based on the physical layer of the IEEE802.15.4-2006 standard in OMNeT++ 4.0 [19]. To achieve this goal, a new developed non beacon enabled MAC layer was used with an IP and UDP layer based on it. This step was necessary because regular IEEE802.15.4 nodes usually imply a network coordinator to synchronize the nodes of the entire network. On the other hand, network coordinators depict a Single-Point-of-Failure (SPOF), which is not desired in safety critical applications. Furthermore, the non beacon enabled MAC layer enables the WSN nodes to perform peer-to-peer communication, which is essential for mesh networks. In addition to that, the IPv4 compliant approach enables various standard applications that are widely-used on the Internet like VoIP or Email. Those VoIP capabilities are appropriate to push voice alarming or warning messages into endangered zones addressed by geocast regions. For a more intelligible comparison of GeoOLSR with various Geocast algorithms, we first analyze only the performance impact of the applied protocols and neglect

PHY layer issues. These effects will be demonstrated in detail in Section VII.

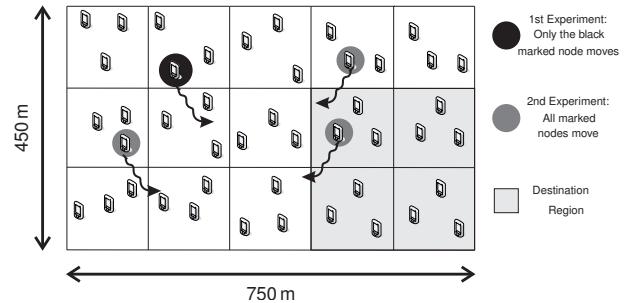


Figure 13. Performance evaluation scenario

A. Validation Scenario

To analyze the performance of GeoOLSR, the following scenario (Figure 13) will be used for all test setups. The scenario measures 750 m x 450 m and consists of 45 nodes distributed homogeneously. To compare GeoOLSR with other geocast algorithms, the source node forwards data into the marked destination zone. In this application scenario the destination region consists of four neighbored zones.

B. Comparison between GeoOLSR and widely used Geocast Algorithms

This section analyzes and evaluates the performance of GeoOLSR with various Geocast algorithms in the scenario mentioned above (cf. Figure 13). In this scenario we omit node mobility and analyze the resulting overhead for a data transmission of 10 kByte from source to the marked destination region. This data transmission is repeated 100 times before a mean value e.g., End-to-End Delay or Transmission Time is calculated. In this experiment the destination region measures 300 m x 300 m and the cell ranges are set to 150 m, which is the maximal free space range of IEEE802.15.4 applying 1 mW transmission power. The results are shown in Table VII.

Table VII
COMPARISON OF THE DIFFERENT GEOCASTING ALGORITHMS

	LBM	flooding GRID	ticket GRID	GeoTORA	GeoOLSR
Effective Data Rate [$kBit/s$]	4.5	12.4	9.8	35	36.2
End-to-End Delay [ms]	45.6	15.2	39.4	12.8	12.8
Transmission Time [s] (UDP Payload = 10 kB)	19.2	7.1	10.7	2.5	2.4
Number of Packets for Transmission	4943	2269	1800	668	648
Overhead [Byte]	14	12	21	4	2
Payload to overall frame size [%]	75.7	78.4	66.2	89.1	91.9
Inherent IP support	no	no	no	no	yes

We observe, that only the route maintaining algorithms support high effective data rates and low end-to-end delays (cf. Section II-B). However, the resulting differences between GeoTORA and GeoOLSR regarding effective data rate and transmission time are caused by our implementation of GeoTORA on ISO-OSI layer 7 whereas GeoOLSR is implemented on ISO-OSI layer 3. Thus, GeoOLSR is able to support slightly higher effective data rates and a little lower transmission time for each delivered packet than GeoTORA. Another important fact that can be omitted is the real time capability of LBM, flooding and ticket based GRID, GeoTORA and GeoOLSR. If we interpret the 10kByte of Payload as a 5 s speech packet (16 kBit/s sampling rate and G.726 voice codec), we see that GeoTORA and GeoOLSR need 2.5 s and 2.4 s respectively to forward this voice alarm message into a certain destination area. In comparison to that LBM and the two GRID derivatives show significant higher transmission times than the original speech length contained in the 10kByte data packet. Hence, we can conclude that only the two route maintaining algorithms are able to support real time simplex voice transmissions. Furthermore, GeoTORA and GeoOLSR are able to save battery lifetime significantly as the overall number of packets needed for the transmission is smaller than the values for LBM, flooding GRID and ticket GRID. Finally, GeoGrid uses 4 Byte for Next Hop, Message Type and Packet Number signaling whereas GeoOLSR uses only 2 Bytes for packet sequence numbering.

Thus, we can postulate that GeoTORA and GeoOLSR are both suited for an application in Wireless Sensor Networks. However, we neglected node mobility until now, which is a very important issue for the aimed application in safety critical scenarios where nodes can exhibit relatively high mobilities. Nevertheless, GeoOLSR depicts two main advantages in comparison to GeoTORA. First, GeoOLSR as a proactive MANET algorithm is able to send an alarm message out immediately from a certain control center, whenever a threatening situation occurs without initiating a previous polling mechanism. Another advantage of GeoOLSR is the simultaneous support of IP-based traffic and location based traffic. That means, no additional geocasting algorithm is needed and the network management is completely integrated in ISO-OSI layer 3.

C. Node Mobility

The previous section neglected nodes' mobility. However, the knowledge of the correct position of each node has a high influence on geocast algorithms. As a quality indicator we regard the position deviation of all fixed nodes between the routing table entry and the real position. That means the difference of the predicted mobile node's position and the real location is calculated for 100 seconds in each node. After that, an overall mean value of the position deviations of all nodes is computed. To allow easier comparability, we

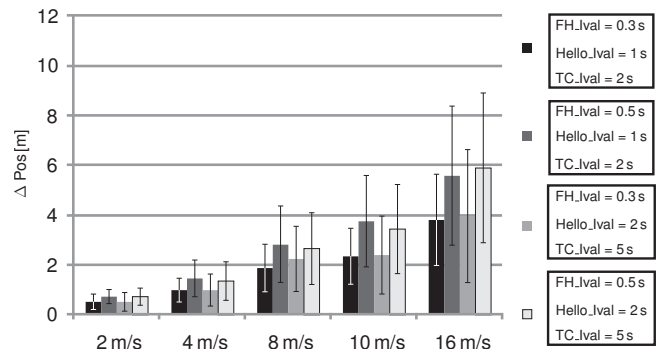


Figure 14. Position Deviation of GeoOLSR depending on varying moving speeds and parameter sets regarding 1 moving node

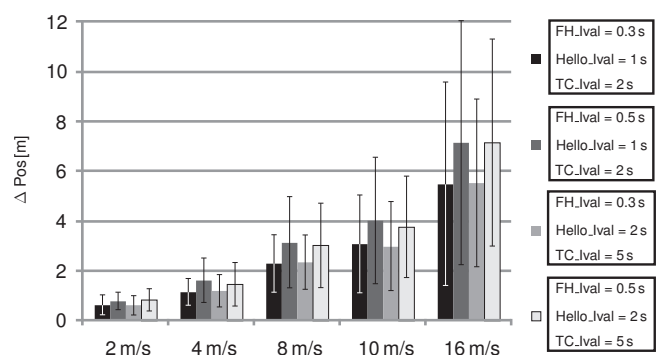


Figure 15. Position Deviation of GeoOLSR depending on varying moving speeds and parameter sets regarding 4 moving nodes

show the same scales for varying motion patterns. In the first experiment, we consider only one node moving around at different speeds. In the second setup, four nodes move through the scenario (cf. Figure 13). The results of the first experiment are shown in Figure 14. The overall mean value of position differences increases as expected with higher node mobility. Here, the same phenomenon can be observed with standard deviations, which indicate a successive rise with higher speeds. However, we can conclude that the ratio of the position deviation to the observed movement speed is always constant. That means, there is a constant average time, in which no communication between nodes is possible due to route maintenance, disconnections etc. Furthermore, we do not see an obvious impact of Hello and TC intervals on position accuracy in contrast to the key parameter Fast Hello interval. As a consequence, position deviation and standard deviation values using equal parameters for Hello and TC interval show nearly the same Δ positions. In the next step we evaluate the influence of higher node mobility within our scenario. Therefore, we compare position deviations of four moving nodes (Figure 15) with those of only one moving node (Figure 14). It is obvious that the increased number of moving nodes does

not have a significant influence on the position accuracy. The difference between position deviations caused by one moving node and four mobile nodes does not exceed 30% when the most network load generating parameters (Fast Hello = 0.3 s, Hello = 1 s and TC = 2 s) are applied at a node speed of 16 m/s. Furthermore, the average increase of position deviations between the one moving node scenario and the four moving nodes scenario is 15.55%. This leads to an important question whether higher route maintaining updates imply higher position accuracies. It is visible that the application of the parameters Fast Hello = 0.3 s, Hello = 2 s and TC = 5 s leads to similar position accuracies like using the parameter set Fast Hello = 0.3 s, Hello = 1 s and TC = 2 s. Due to battery and resource constraints it is advisable to use the parameter set with lower Hello and TC intervals as this approach saves battery life and decreases the number of collisions.

D. Analysis of resulting overheads

In this section, we will analyze the overhead evoked by GeoOLSR in comparison to regular OLSR. The test scenario is the same as shown in Figure 13. As a reference, regular OLSR is considered without geocasting functionalities. In this experiment we consider one moving node and four moving nodes for two different OLSR parameter sets. Here, we neglect varying speeds as GeoOLSR only uses time triggered route maintenance packets, which are independent of different speeds. The results are shown in Table VIII.

Table VIII
RESULTING OVERHEADS COMPARED TO REGULAR OLSR

regular OLSR with 45 static nodes			
OLSR	44.42 kBit/s		
GeoOLSR	1 moving Node	4 Moving nodes	
Fast Hello = 0.3 s	60.88 kBit/s	79.5 kBit/s	
Fast Hello = 0.5 s	51.57 kBit/s	71.94 kBit/s	

Hello Interval = 1 s
TC Interval = 2 s

regular OLSR with 45 static nodes			
OLSR	25.61 kBit/s		
GeoOLSR	1 moving Node	4 Moving nodes	
Fast Hello = 0.3 s	51.42 kBit/s	72.69 kBit/s	
Fast Hello = 0.5 s	42.29 kBit/s	65.74 kBit/s	

Hello Interval = 2 s
TC Interval = 5 s

In contrast to Section III, we did not evaluate goodputs here, because the use of the random mobility model leads to fluctuating goodput values and are not comprehensible due to variable hop distances between source and sink.

We see that even the most accurate parameter set shows an overhead of 35.08 kBit/s (OLSR compared to GeoOLSR with *Fast Hello Interval* = 0.3 s and 4 moving nodes). Furthermore, the overhead of one moving node compared to 4 moving nodes is in-between 18.62 and 23.45 kBit/s (*Fast Hello Interval* = 0.3 s versus *Fast Hello Interval* = 0.5 s).

Thus, even in the most data rate consuming parameterization there are still 170.5 kBit/s left for payload traffic.

VII. PERFORMANCE EVALUATION IN A REAL WORLD ENVIRONMENT

Industrial scenarios pose a challenging network environment for IEEE802.15.4 networks due to the special fading conditions. In order to analyze the performance of protocols and applications, network simulators like OMNeT++ only apply a deterministic free space loss propagation model. This model, however, poorly reflects the channel characteristics of real world conditions. Therefore, a sophisticated ray tracing tool (Radiowave Propagation Simulator) is used to represent shadowing effects and multipath propagation. To increase accuracy of the simulation results, we used a 3D laser scan for creating a CAD model of the scenario, which considers every pipe, tube and steel girder included in the observed basements underneath a batch annealing plant of a ThyssenKrupp cold rolling mill (cf. Figure 16).

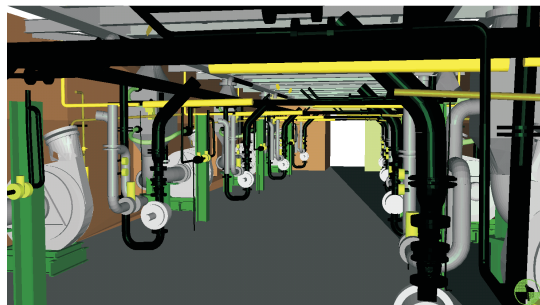


Figure 16. Top: Image of the supply machinery basement underneath the analyzed cold rolling mill. Bottom: Detailed 3D CAD model of the scenario shown above.

The combination of a highly detailed CAD model with ray tracing allows an accurate determination of Received Signal Strength Indicator (RSSI) values as well as Signal to Noise plus Interference Ratios (SNIR). IEEE802.15.4a-CSS, as applied in the gas concentration monitoring scenario for employee localization in case of emergency, possesses a minimal RSSI value of -95 dBm and a minimal SNIR of -17 dB. Hence, we modified the applied OMNeT++ PHY

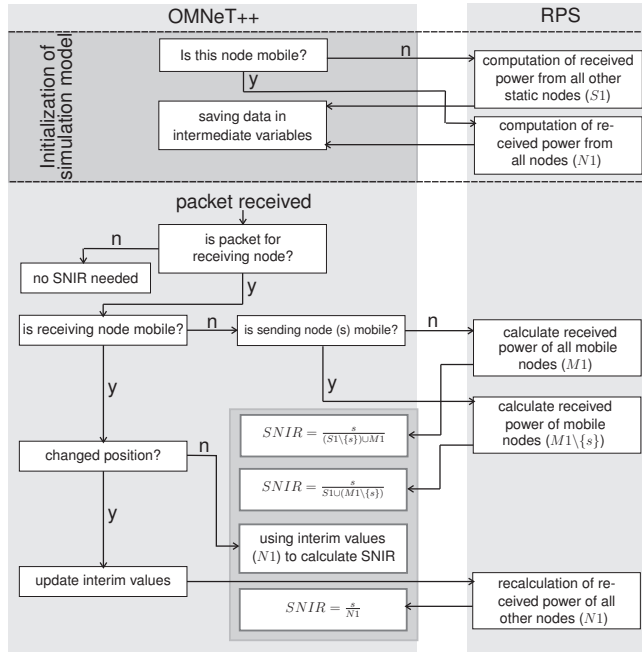


Figure 17. Simulation Architecture consisting of OMNeT++ and Radiowave Propagation Simulator (RPS) to increase PHY layer modeling accuracy. For computational time reduction, two intermediate result sets ($S1$ and $N1$) are applied during initialization period of the OMNeT++ model.

layer implementation to discard incoming packets that do not exhibit these minimum values and extended it with a direct connection to the ray tracing tool. However, to reduce computational complexity, we perform a special SNIR computation, in which two different intermediate results are saved, which may be reused on every SNIR calculation. The simulation architecture is shown in Figure 17. During initialization of OMNeT++, the sum of all adjacent stationary nodes is calculated for each non mobile node ($S1$) (anchor nodes that are mounted to the wall), whereas the received power of all adjacent nodes is cumulated for every mobile node in the scenario ($N1$). The intermediate value of each stationary node remains constant during simulation process and must be modified by the sum of all mobile nodes ($M1$) that do not participate in the observed communication process. $M1$ must be recomputed every time a SNIR value is requested by the PHY layer due to the mobility of this node set and the consecutive changes in RSSI and SNIR values. To reduce the amount of computational steps once again, the intermediate result set $N1$ is updated every 1 m only. The applied movement paths are shown in Figure 18.

In this setup, we apply a radio channel, which occupies 80 MHz of bandwidth with a center frequency of 2.45 GHz as our installed localization tags and anchor nodes use IEEE802.15.4a-CSS. Furthermore, we use dipole antennas with 2.2 dB gain and a transmission power of 0 dBm. The sent traffic profile applies packets encapsulating a payload

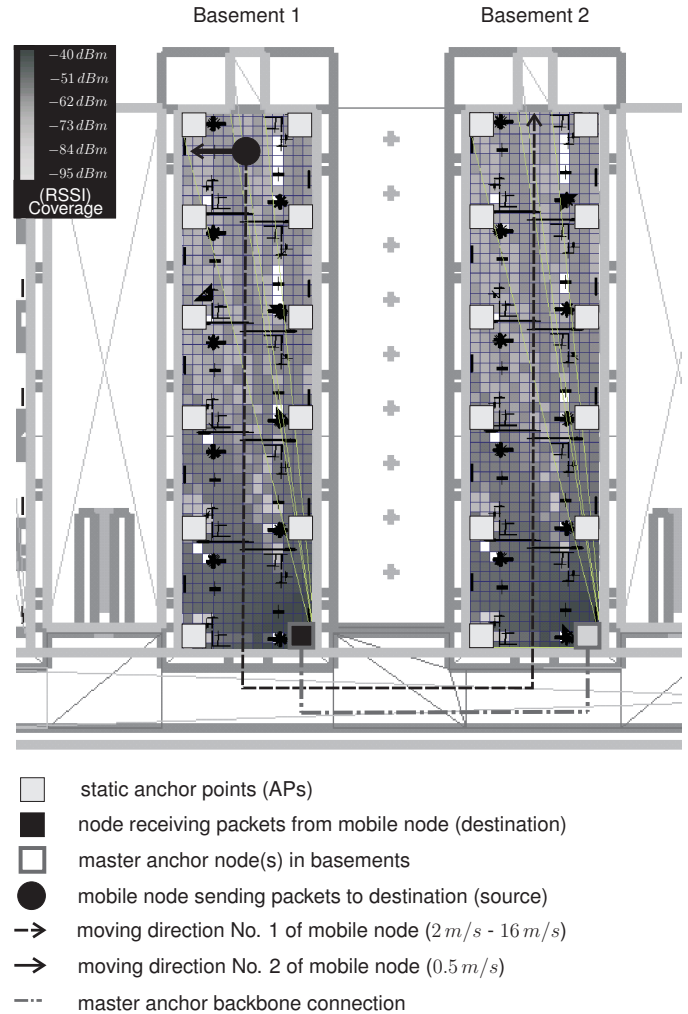


Figure 18. Applied moving direction of a mobile node which sends data to a static anchor point (AP). The other APs depict potential interferers in the observed positioning system.

of 74 Byte with an interarrival time of 30 ms (as applied in the evaluations before). First, we analyze the resulting goodput for different speeds in this scenario (cf. Figure 19) including a basement change (moving direction No. 1) and an exemplary maintenance of an anchor point (moving direction No. 2). During maintenance of machinery or stationary anchor points the service employees might be shadowed by surrounding tubes or pipes. Here, reliable handover processes must ensure connectivity of the mobile personnel.

As the scenario omits a very good radio coverage (as shown in Figure 18), there are only connections with a maximal 2 hop distance between source and destination. However, the resulting SNIR affect the radio channel significantly. Hence, the main influencing factor for the resulting goodputs of the first four measurements (0.5 m/s, 2 m/s, 4 m/s and 8 m/s) is multipath propagation (for both desired

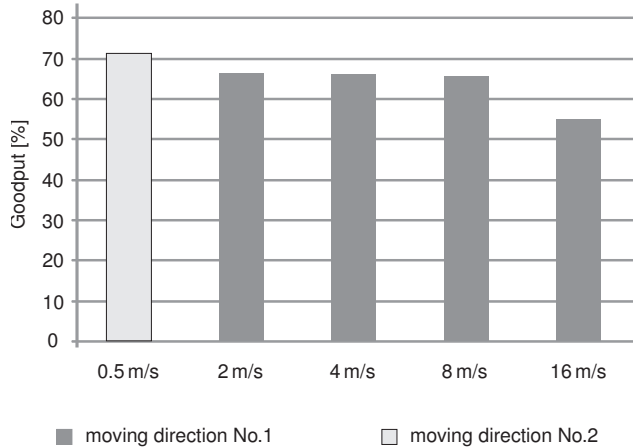


Figure 19. Resulting Goodput of GeoOLSR depending on varying moving speeds and parameter sets regarding 1 moving node under real-world channel conditions. ($FH_Ival = 0.5\ s, HI = 2\ s, TC_Ival = 5\ s$)

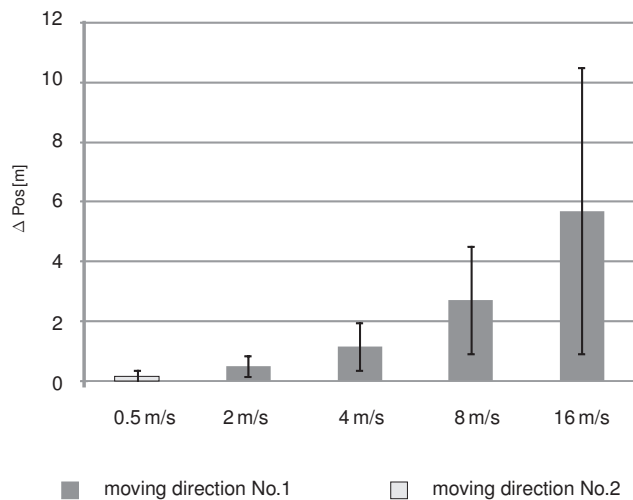


Figure 20. Position Deviation of GeoOLSR depending on varying moving speeds and parameter sets regarding 1 moving node under real-world channel conditions. ($FH_Ival = 0.5\ s, HI = 2\ s, TC_Ival = 5\ s$)

connections and undesired interference signals). Here, we only show exemplary results in Figure 19 without declaration of mean values or standard deviations. Compared to the original OMNeT++ analysis of OLSR (cf. Figure 6), a 20% worse result is achieved considering the 1 and 2 hop cases. The 16 m/s measurement is subject to the increased speed as well as in the original OMNeT++ simulation. Nevertheless, the goodputs are still satisfying in such a scenario if low pedestrian speeds are assumed. Usual movement speeds for employees would be around 1 m/s up to 2 m/s.

Another important metric for safety critical localization systems is the position deviation as analyzed in Section V. The position deviation of GeoOLSR in a real-world scenario (Figure 20) is nearly equal to the previous scenario setup (Figure 14). This may be explained by the slightly reduced

maximal hop count in the real-world scenario compared to the original measurement in Section VI. Furthermore, the deviation is still relatively small for low mobility speeds, which are typical due to the construction type of industrial environments where fast movements of employees do not occur frequently. Thus, fast evacuation is ensured as the resulting position deviations correspond an "arm's length" (for mobility speeds of up to 2 m/s), which enables firemen to rescue people quickly and reliable even if sight is limited.

VIII. CONCLUSION

We presented a novel peer-to-peer enabled IEEE802.15.4 node design for meshed network topologies and compared it against the original IEEE802.15.4 solution. We have seen that the energy consumption of our GeoOLSR nodes is about 3 times higher (3297 minutes) than the energy optimized end devices of the IEEE802.15.4 standard (10416 minutes), but the lifetime is enhanced in comparison to IEEE802.11 (55 minutes). The major advantage of the node is the enhanced fault tolerance against node failures and the autonomous reconfiguration capability. The routing algorithms provide good performance in handover processes in terms of switching times and goodput.

Subsequently, we also outlined a geocasting algorithm based on Optimized Link State Routing (OLSR) that is able to support high mobilities at a reasonable traffic overhead. Due to the proactive nature of the underlying OLSR protocol this extension is well suited for real time alarming services in safety critical scenarios, which do not permit an additional polling mechanism e.g., if danger zones must be evacuated immediately.

The deployment of IP in wireless sensor networks enables an easy integration of sensor nodes into preexisting infrastructures, without the need of special gateways, as well as a wide variety of services, which are widely accepted within the Internet community. Finally, GeoOLSR is able to use IP-based unicast traffic as well as location based services without the need of an additional geocasting algorithm beside the applied mesh network algorithm.

ACKNOWLEDGMENT

This work is conducted within the SAVE Project (Geographic Information System for Alarming using autonomous, networked Gas Sensors) and is funded by the German Federal Ministry of Education and Research (BMBF) – 16SV3711

REFERENCES

- [1] A. Lewandowski, V. Koester, and C. Wietfeld: *Performance Evaluation of AODV- and OLSR-meshed IP-enabled IEEE802.15.4*, 2010 Third International Conference on Advances in Mesh Networks (MESH 2010), Venice, Italy, July 2010
- [2] C. Perkins, E. Royer, and S. Das: *Ad hoc On-Demand Distance Vector (AODV) Routing*, IETF RFC 3561, 2003
- [3] T. Clausen and P. Jacquet: *The Optimized Link State Routing Protocol (OLSR)*, IETF RFC 3626, October 2003
- [4] Z. Shelby and C. Bormann: *6LoWPAN: The wireless Embedded Internet*, John Wiley & Sons Ltd, ISBN: 978-0-470-74799-5, 2009
- [5] ZigBee Alliance. ZigBee Specification. Technical Report Document 053474r17, Version 1.0, ZigBee Alliance, October 2007
- [6] J. W. Hui and D. E. Culler: *IP is dead, long live IP for wireless sensor networks*, In Proceedings of the 6th ACM Conference on Embedded Network Sensor Systems (SenSys '08), Raleigh, NC, USA, November 2008
- [7] A. Dunkels, T. Voigt, and J. Alonso: *Making TCP/IP Viable for Wireless Sensor Networks*, In Proceedings of the First European Workshop on Wireless Sensor Networks (EWSN 2004), Berlin, Germany, January 2004
- [8] K. Kim, S. D. Park, G. Montenegro, and S. Yoo: *6LoWPAN Ad Hoc On-Demand Distance Vector Routing (LOAD)*, draft-daniel-6lowpan-load-adhocrouting-01, IETF Internet Draft (Work in progress), July 2005
- [9] J. Deissner, J. Huebner, D. Hunold, and J. Voigt: *RPS Radiowave Propagation Simulator*, User Manual, www.actix.com, last visited June 2011
- [10] D. B. Johnson, D. A. Maltz, and Y.-C. Hu: *The Dynamic Source Routing Protocol (DSR) for Mobile Ad Hoc Networks for IPv4*, IETF RFC 4728, February 2007
- [11] S. Hamma, E. Cizeron, H. Issaka, and J.-P. Guedon: *Performance evaluation of reactive and proactive routing protocol in IEEE 802.11 ad hoc network*, In Proceedings of ITCOM 06, Boston, MA, USA, October 2006
- [12] M. Benzaid, P. Minet, and K. Alagha : *Integrating fast mobility in the OLSR routing protocol*, 4th IEEE Conference on Mobile and Wireless Communications Networks , Stockholm, Sweden, September 2002
- [13] C. Gomez, P. Salvatella, O. Alonso, and J. Paradells: *Adapting AODV for IEEE802.15.4 mesh sensor networks: theoretical discussion and performance evaluation in a real environment*, 2006 International Symposium on World of Wireless, Mobile and Multimedia Networks (WoWMoM 2006), pp. 159 - 170, Buffalo, NY, USA, June 2006
- [14] Y.-B. Ko and N.H. Vaidya: *GeoTORA: a protocol for geocasting in mobile ad hoc networks*, In Proceedings of the International Conference on Network Protocols, pp. 240-250, Osaka, Japan, November 2000
- [15] W.-H. Liao, Y.-C. Tseng, K.-L. Lo, and J.-P. Sheu : *GeoGrid: A Geocasting protocol for mobile ad hoc networks based on grid*, Journal of Internet Technology, pp. 23-32, 2000
- [16] Y.-B. Ko and N.H. Vaidya: *Geocasting in Mobile Ad Hoc Networks: Location-Based Multicast Algorithms*, In Proceedings of the Second IEEE Workshop on Mobile Computer Systems and Applications (WMCSA 1999), Washington, DC, USA, 1999
- [17] D. Camara and A. Loureiro: *A Novel Routing Algorithm for Ad Hoc Networks*, Baltzer Journal of Telecommunications Systems, Kluwer Academic Publishers, vol. 18:1-3, pp. 85-100, 2001
- [18] B. Zhou, F. De Rango, M. Gerla, and S. Marano: *GeoLAN-MAR: geo assisted landmark routing for scalable, group motion wireless ad hoc networks*, IEEE 61st Semiannual Vehicular Technology Conference (VTC), Stockholm, Sweden, 2005
- [19] A. Varga: *The OMNeT++ Discrete Event Simulation System*, In Proceedings of the European Simulation Multiconference, 2001
- [20] Wireless Medium Access Control (MAC) and Physical Layer (PHY) Specifications for Low-Rate Wireless Personal Area Networks (WPANs), IEEE802.15.4 (Standard), 2006
- [21] A. Kiryushin, A. Sadkov, and A. Mainwaring: *Real-World Performance of Clear Channel Assessment in 802.15.4 Wireless Sensor Networks*, 2008 Second International Conference on Sensor Technologies and Applications (SENSORCOMM 2008), pp. 625-630, Cap Esterel, France, August 2008
- [22] A. Lewandowski, M. Putzke, V. Koester, and C. Wietfeld: *Coexistence of 802.11b and 802.15.4a-CSS: Measurements, Analytical Model and Simulation*, 71st IEEE Vehicular Technology Conference (VTC), Taipei, Taiwan, May 2010
- [23] Y. Huang, S. N. Bhatti, and D. Parker; *Tuning OLSR*, 2006 IEEE 17th International Symposium on Personal, Indoor and Mobile Radio Communications (PIMRC 2006), pp. 1-5, September 2006
- [24] I. D. Chakeres and L. Klein-Berndt: *AODVjr, AODV simplified*, ACM, SIGMOBILE Mob. Comput. Commun. Rev., vol. 6, no.3, pp. 100-101, 2002 doi: <http://doi.acm.org/10.1145/581291.581309>, last visited June 2011
- [25] Texas Instruments CC2420 Single-Chip 2.4 GHz IEEE 802.15.4 RF Transceiver, Datasheet, <http://focus.ti.com/docs/prod/folders/print/cc2420.html>, last visited June 2011
- [26] Maxim MAX2822 2.4 GHz IEEE 802.11b RF Transceiver, Datasheet, <http://www.maxim-ic.com/datasheet/index.mvp/id/3938>, last visited June 2011